Macroscopic Highly Aligned DNA Nanowires Created by Controlled Evaporative Self-Assembly

Bo Li,[†] Wei Han,[†] Myunghwan Byun,[‡] Lei Zhu,[§] Qingze Zou,[⊥] and Zhiqun Lin[†,*]

[†]School of Materials Science and Engineering, Georgia Institute of Technology, Atlanta, Georgia 30332, United States, [‡]Department of Polymer Science and Engineering, University of Massachusetts, Amherst, Massachusetts 01002, United States, [§]Department of Macromolecular Science and Engineering, Case Western Reserve University, Cleveland, Ohio 44106, United States, and [⊥]Department of Mechanical and Aerospace Engineering, Rutgers the State University of New Jersey, Piscataway, New Jersey 08854, United States

ABSTRACT By subjecting DNA aqueous solution to evaporate in a curve-on-flat geometry that was composed of either a spherical lens or a cylindrical lens situated on a flat substrate, a set of highly aligned DNA nanowires in the forms of spokes and parallel stripes over a macroscopic area (*i.e.*, millimeter scale) were successfully created. The DNA molecules were stretched and aligned on polymer-coated substrate by the receding meniscus. The imposed curve-on-flat geometry provided a unique environment for controlling the flow within the evaporating solution by eliminating temperature gradient and possible convective instability and, thus, regulated the formation of DNA nanowires. Such controlled evaporative self-assembly is remarkably easy to implement and opens up a new avenue for crafting large-scale DNA-based nanostructures in a simple and cost-effective manner, dispensing with the need for lithography techniques.

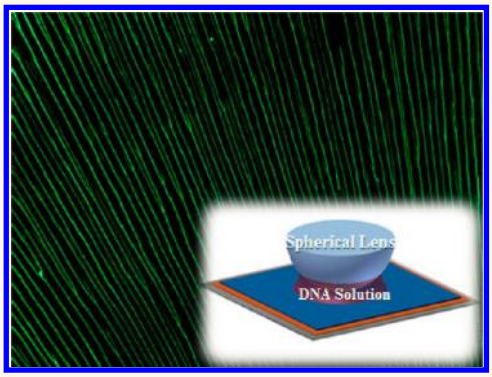

KEYWORDS: DNA nanowire · controlled evaporation self-assembly · confined geometry

DNA is a promising construction material for producing well-defined nanostructures for electronic, magnetic, optoelectronic, and sensory applications. In particular, DNA nanowires produced by stretching DNA permit the physical mapping and diagnosis of diseases,[1] and can also serve as unique templates due to their aligned structure and rich chemical functionality[2] for potential use in superconducting nanowires,[3] waveguides,[4] photodetection,[5,6] field-effect transistor,[7] nanophotonic switch,[8] biosensors,[9] nanowire transistor,[10] thermal switch,[11] logic device,[12] *etc.* Notably, the prerequisite for most of these applications involving DNA nanowires is to immobilize a large number of DNA molecules on the substrate at the desired position. To date, several methods stemming from simple molecular combing approach,[1] including air blowing,[13] electrophoretic stretching,[14] spin-stretching,[15] combing in microchannels,[16] and dynamic molecular combing[17] have been utilized to align and immobilize coiled DNA molecules onto the substrate. Under certain pH and ionic strength, the partial melting of the ends (*i.e.*, extremities) of DNA molecules exposes their hydrophobic core, which adsorbs onto a hydrophobic surface (*i.e.*, specific binding).[16,18] In general, the stretched DNA chains were often randomly distributed. They are not well positioned and ordered over a large area. The length of DNA molecules was also not controlled. Recently, the parallel alignment of DNA arrays has been achieved using a modified molecular combing method combined with soft lithography (*i.e.*, placing a PDMS stamp in contact with the DNA solution);[19,20] however, the process was rather complex in terms of the mask preparation and requiring delicate control over the peeling-off speed of PDMS stamp. By utilizing solvent evaporation on a tilted PDMS surface, DNA nanofibers can be fabricated; however, the effects of temperature and pH on the nanofiber formation are still not well understood.[21] Clearly, a low-cost, large-scale strategy for highly aligned DNA nanowires is highly desirable and requires a thorough and systematic study.

* Address correspondence to zhiqun.lin@mse.gatech.edu.

Received for review February 19, 2013 and accepted April 3, 2013.

Published online April 04, 2013
10.1021/nn400840y

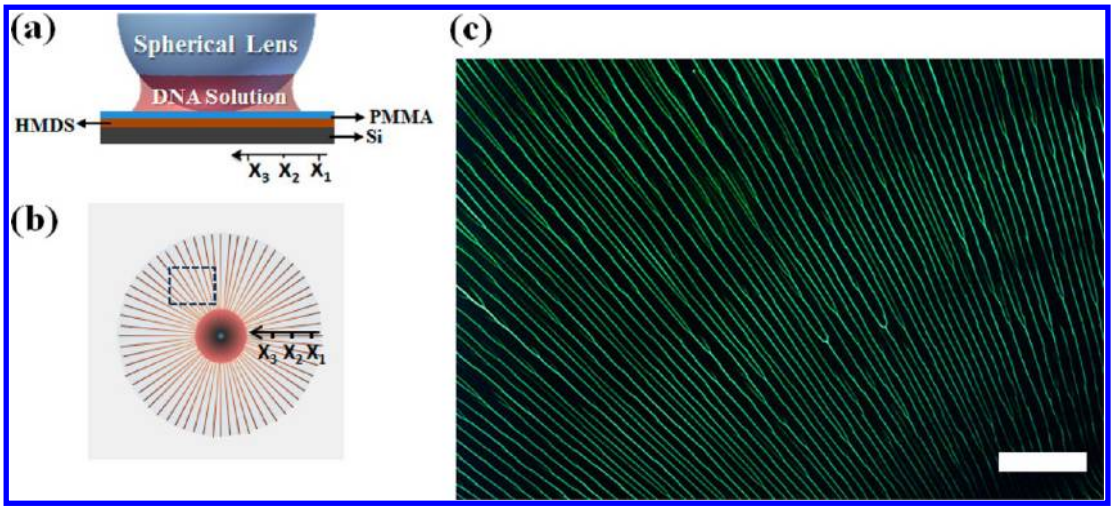

Figure 1. (a) Schematic illustration of sphere-on-flat geometry (side view), where a drop of DNA solution is constrained, bridging the gap between the spherical lens and the PMMA-coated Si substrate (*i.e.*, a thin PMMA film was spin-coated on HMDS-coated Si). (b) Schematic illustration of formation of DNA spokes (top view). (c) A small zone of DNA spokes obtained at pH = 6.2, T = 65 °C, and the concentration of DNA solution = 8 μg/mL (marked as a dashed box in panel b), emitting green fluorescence. Scale bar = 300 μm.

The use of spontaneous self-assembly as a lithography- and external field-free means to construct highly ordered, often intriguing structures has garnered much attention due to the ease of producing complex, large-scale structures with small feature sizes. In this regard, one extremely simple route to intriguing structures is the drying-mediated self-assembly of nonvolatile solutes (*e.g.*, polymers, nanoparticles and colloids) through the solvent evaporation of a sessile droplet on a solid substrate.[22] However, the flow instabilities within drying droplet often result in non-equilibrium and irregular dissipative structures (*e.g.*, randomly organized convection patterns, stochastically distributed multirings, and so on). To this end, controlled evaporative self-assembly in a confined geometry has recently emerged as a rational preparation strategy for simple and rapid creation of well-ordered microscopic structures,[22] comprising polymers[23−26] and particles.[27] The confined geometry imparts a radically distinctive environment for exquisite control over the evaporation process (*e.g.*, evaporative flux, solution concentration, interfacial interaction between the solute and substrate, *etc.*) to yield complex structures and assemblies with high regularity and fidelity.

Herein, we demonstrate a *simple yet robust* strategy to yield highly aligned parallel DNA nanowires in the forms of nanostructured spokes and parallel stripes *over a macroscopic area* (*i.e.*, *millimeter scale*) by subjecting DNA aqueous solution to evaporate in a curve-on-flat geometry composed of either a spherical lens or a cylindrical lens situated on a flat substrate. Such confined geometry allowed for the control over the flow within the evaporating solution by eliminating temperature gradient and possible convective instability, thereby leading to the stretching of DNA molecules by the receding meniscus, and in turn forming highly ordered DNA nanowires. The effects of pH of DNA aqueous solution and temperature on the formation of DNA nanowires were systematically explored. A transition from spoke-like patterns to coffee-ring-like deposits was, for the first time, observed as the pH was increased. The optimization of pH and temperature rendered the production of large-scale DNA nanowires aligned parallel to one another.

RESULTS AND DISCUSSION

The DNA spoke-like patterns were formed by allowing a drop of λ-DNA (hereafter referred to as "DNA") aqueous solution to evaporate in sphere-on-flat geometry constructed by placing a spherical lens on a flat PMMA-coated Si substrate (Figure 1a; see Experimental Section). The PMMA-coated Si substrate was hydrophobic and facilitated the anchoring of DNA on its extremity. The formation of DNA spokes, analogous to aligning seaweeds on the beach during ebb-tide, can be understood as follows. At the early stage of the drying process, the fingering instabilities caused by the long-range van der Waals force between the liquid and the substrate[28] occurred at the drying front of the DNA aqueous solution. DNA molecules were preferably accumulated at the fingers. Over a certain range of pH, the extremities of DNA were then anchored at the three-phase contact line on the PMMA-coated substrate as a result of the interaction of the extremities with the carboxyl group of PMMA;[1,18] such anchoring was strong enough to withstand the capillary force (*i.e.*, combing force[29,30]). The DNA molecules were stretched straight due to the capillary force acting on the rest of DNA molecules by the receding solution front (*i.e.*, air/water interface) during the water evaporation.[31] The anchored DNAs served as nucleation sites and grew into stripes locally that oriented normal

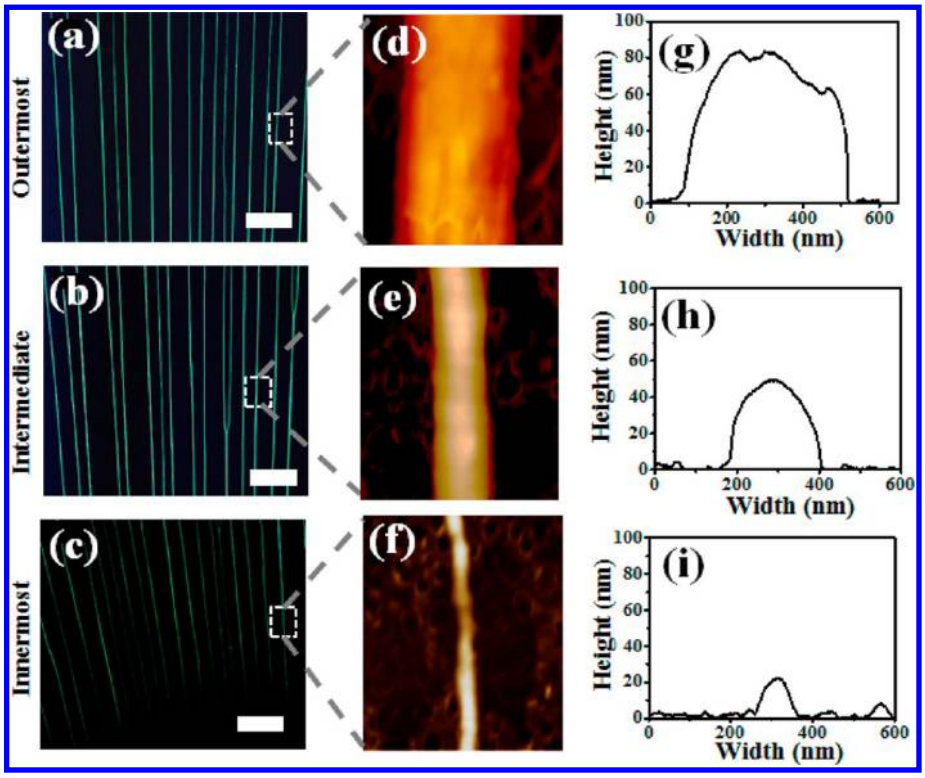

Figure 2. (a−c) Representative fluorescence micrographs of DNA spokes formed at three different regions (*i.e.*, (a) outermost region, X_1; (b) intermediate region, X_2; and (c) innermost region, X_3) obtained at pH = 6.2, T = 65 °C, and the concentration of DNA solution = 8 μg/mL. (d−f) AFM height images of selected areas in panels a−c; image size = 600 nm × 600 nm. (g−i) The corresponding cross-sectional analysis of AFM images of DNA spokes in paneld d−f.

to the evaporating front by transporting DNAs from the surrounding solution as the solution front (*i.e.*, meniscus) propagated inward. This resulted in spoke patterns (Figure 1b).[32]

To scrutinize the surface morphology of the DNA spokes, optical microscopy and AFM measurements were performed. The spacing between two adjacent DNA spokes did not change much from the outermost region (X_1 in Figure 1a,b) to the innermost region (X_3 in Figure 1a,b) as the solution front moved toward the sphere/PMMA-coated Si contact center (Figure 1). This is because as the perimeter of the three-phase contact line dictated by the spherical lens decreased from X_1 to X_3 regions, the spacing between two adjacent DNA spokes is expected to decrease; however, the two adjacent spokes may merge together as one spoke if the distance between them at the drying front was close enough. Locally, the height, h, and width, w, of DNA spokes were constant. However, they progressively (but not continuously as will be discussed later) decreased from the outermost region X_1 to the innermost region X_3 as evidenced in three representative AFM height images and the corresponding cross-sectional analysis, namely, from h = 80 nm and w = 400 nm at X_1 = 4200 μm (Figure 2d.g), to h = 50 nm and w = 200 nm at X_2 = 3400 μm (Figure 2e,h), and to h = 20 nm and w = 100 nm at X_3 = 2600 μm (Figure 2f,i); this is not surprising as less DNA molecules were available to be transported to the meniscus as the evaporation proceeded from X_1 to X_3 (Figure 1a,b).[33] Obviously, the use of sphere-on-flat geometry rendered the production of DNA spokes over a large area (Figure 1c and 2a,c) with a very long distance (*i.e.*, approximately from X_1 = 2600 μm X_3 = 4200 μm, so a total of 1.6 mm long) (Figure 1c). On the basis of these observations, it is clear that the dimension of DNA nanowires (*i.e.*, spokes formed in sphere-on-flat geometry) was dictated by not only the concentration of DNA solution, but also the geometry of the upper spherical lens used.

As noted above, the length of a complete DNA spoke was approximately 1.6 mm, which was also measured by AFM (Figure 3). It is noteworthy that the maximum achievable length of DNA spokes is simply limited by the diameter of upper spherical lens used (D = 1 cm in Figure 1a) and the volume of DNA solution loaded. It can be expected that by increasing D and placing a larger amount of DNA solution, much longer DNA spokes with even larger areas can be readily yielded.

Interestingly, although the overall trend of height h of DNA spokes decreased from X_1 to X_3 as described above, such decrease was not continuous. Instead, a fluctuation in h along a DNA spoke was seen, indicating that during the drying of DNA solution, the three-phase contact line moved toward the sphere/PMMA-coated Si contact center in a "*slow-and-fast*" manner (Figure S1). The underlying mechanism for such "*slow-and-fast*"

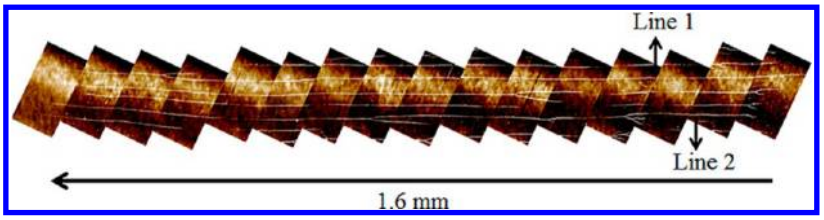

Figure 3. Representative AFM image of complete DNA spokes with a total length of 1.6 mm formed at pH = 6.2, T = 65 °C, and the concentration of DNA solution = 8 μg/mL. The arrow marked the direction of drying front during the course of water evaporation. The cross-sectional analysis of Line 1 and Line 2 is summarized in Figure S1.

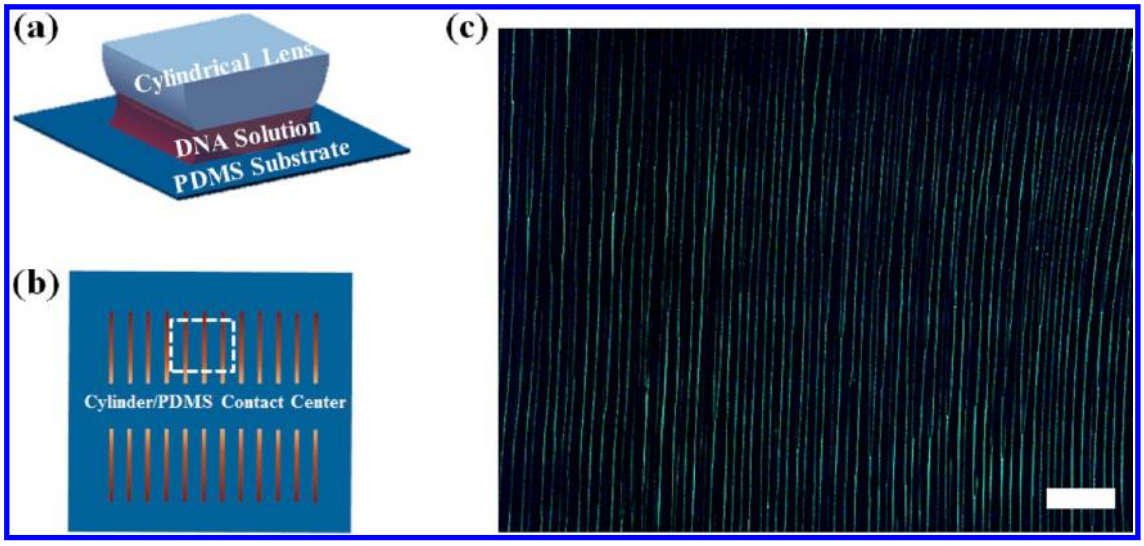

Figure 4. (a) Schematic illustration of cylinder-on-flat geometry composed of a cylindrical lens situated on a PDMS substrate (side view). (b) Schematic illustration of formation of parallel DNA stripes on two sides of the cylinder/PDMS contact (marked as "cylinder/PDMS contact center"); similar illustrations are shown in Figure 5a. (c) A small zone of parallel DNA stripes (marked as white dashed box in panel b) yielded at pH = 6.2, T = 65 °C, and the concentration of DNA solution = 8 μg/mL, emitting green fluorescence. Scale bar = 200 μm.

motion of the meniscus may be rationalized as follows. During the spoke formation process, it was highly possible that the concentration of DNA solution may increase with time due to water evaporation (*i.e.*, the "*slow*" motion period). As such, the DNA spokes may grow thicker as more DNA were dragged and bundled to the existing DNA nucleation sites, which in turn slowed down the deposition process. The slow move of meniscus further increased the thickness of DNA spokes (*i.e.*, the positive slope in the *Height* ~ *Distance* plot in Figure S1; upward). Subsequently, the "*fast*" motion was followed. This is because after a certain period of the "*slow*" motion, the concentration of DNA solution decreased as most of DNA was deposited during this period, leading to the formation of thinner DNA spokes and the increased moving speed of meniscus. The fast moving of drying front resulted in further decrease in the thickness of DNA spokes (*i.e.*, the negative slope in the *Height* ~ *Distance* plot in Figure S1; downward), which led to an increase in the concentration of DNA solution. As the concentration increased, the condition for the "*slow*" motion was satisfied; the DNA spokes would grow thicker again. Clearly, the repeated "*slow-and-fast*" motion of drying front resulted in the height fluctuations along DNA spokes, as also represented in the alternation in fluorescence intensity of green emitting dye-labeled DNA (Figure 1c).

The pH value was found to exert a profound influence on the alignment of DNA molecules. The anchoring of DNA on substrate was sensitive to pH, and different pH of DNA solution was responsible for a specific binding mechanism of DNA.[18,34] For a given temperate T = 65 °C, at low pH (*i.e.*, pH = 5.5 in Figure S2a), the DNA molecules were either randomly deposited or aggregated during water evaporation. This is because DNA molecules underwent intensive protonation, which induced strong nonspecific absorption of DNA on the PMMA surface (*i.e.*, PMMA-coated Si substrate). As the capillary force (*i.e.*, combing force) of drying front was small as compared to the large anchoring force between DNA and the PMMA surface, the meniscus was not able to straightly stretch DNA molecules as it receded. Thus, instead of highly aligned DNA spokes, branches and junctions of DNA spokes were formed. When pH increased to 5.8−6.4 (*e.g.*, optimal pH = 6.2 in Figure S2b) as in the present study, the denaturation of DNA disappeared and was only restricted to its extremities. Thus, instead of the midsegment of DNA, DNA molecules were anchored by the end. Subsequently, DNA molecules were aligned (*i.e.*,

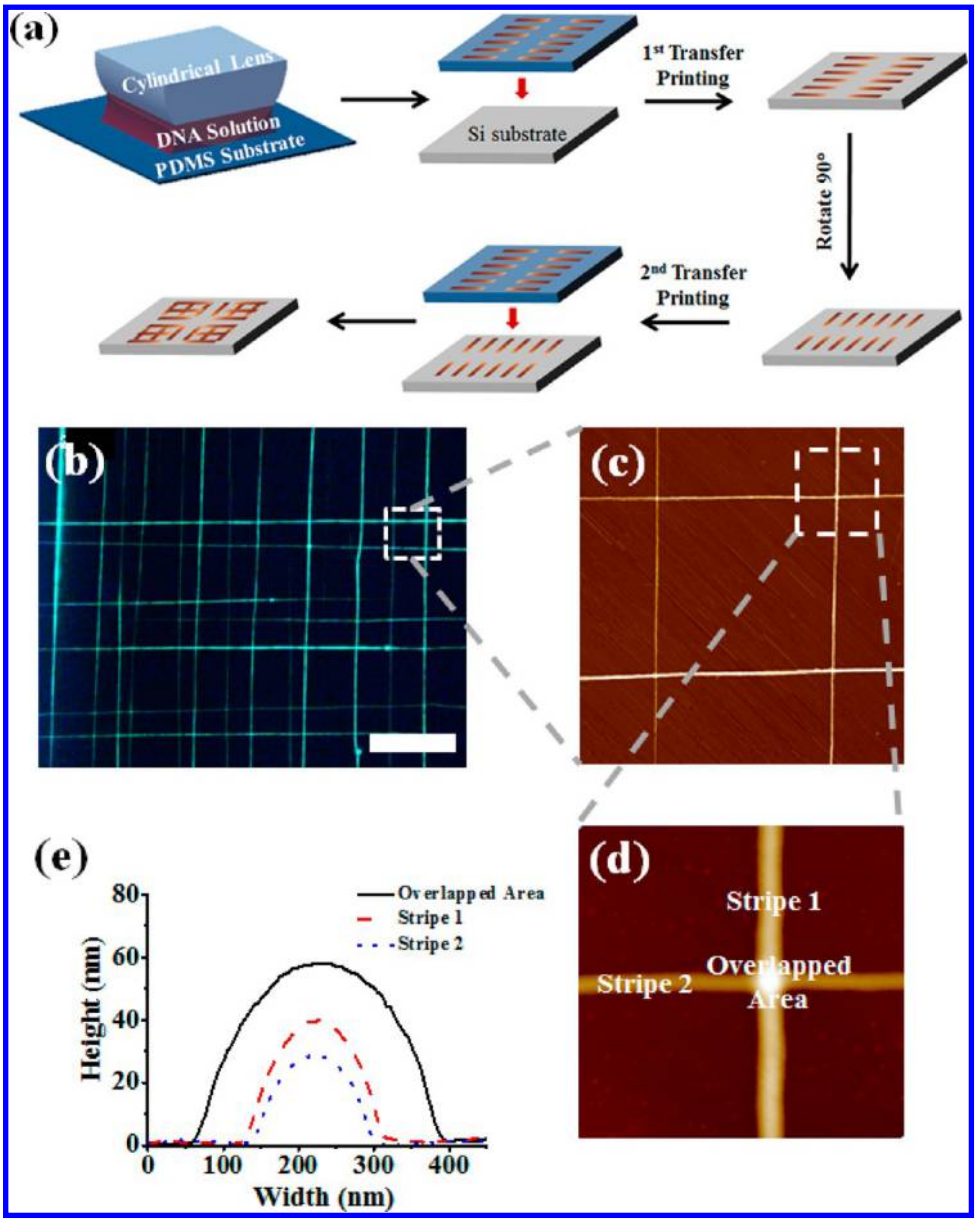

Figure 5. (a) Schematic representation of preparation of 2D arrays of DNA nanowires by two consecutive orthogonal transfer-printing using PDMS substrate. The parallel DNA stripes (*i.e.*, a set of lines on the left and right sides in the 2nd and 5th upper panels) were formed on two sides of the cylinder/PDMS contact center. (b) Representative fluorescence micrograph of 2D arrays of DNA nanowires; scale bar = 40 μm. (c) AFM height image of a selected area in panels b; image size = 20 μm $\times$ 20 μm. (d) The close-up of an overlapped area in panel c; image size = 20 μm $\times$ 20 μm. (e) The corresponding height profiles of stripe 1, stripe 2, and overlapped area in panel d.

forming DNA spokes) by the capillary force acting on the rest of DNA molecules as the meniscus receded,[31] as discussed earlier in the above. When pH increased to a higher value (*e.g.*, pH = 7.1 in Figure S2c), little DNA denaturation occurred; in other words, the anisotropic property of DNA molecules vanished, and the weak binding between DNA and the PMMA-coated Si substrate cannot fix DNA to the surface. Consequently, DNA can be regarded as a conventional polymer with a large length to diameter aspect ratio. Thus, it is not surprising that concentric ring-like structures were yielded due to "*stick–slip*" motion of three phase contact line, resembling our previous work on dynamic self-assembly of polymers.[22,23,25−27,33] Notably, a transition from spoke-like patterns (pH = 6.2) to coffee-ring-like deposits (pH = 7.1) was thus, for the first time, observed as pH increased.

In addition to pH, the effect of temperature, which was much less studied in previous molecular combing-based approaches, on the stretching and alignment of DNA was also explored. We note that (a) an increase in temperature would lead to a higher evaporation rate of solvent, and thus faster receding of the three-phase contact line, which in turn promotes the alignment of DNA molecules at the drying front; and (b) on the other hand, the increase in temperature would facilitate the

convective flow that carries DNA molecules from the solution inside to the drying front, that is, more DNA would deposit at the three-phase contact line.[33,35] Clearly, based on our observation at the fixed pH = 6.2 as displayed in Figure S2d−f, the formation of DNA spokes were more likely governed by the former (*i.e.*, (a)). At relatively low temperature (*i.e.*, $T \leq 55$ °C in Figure S2d), the meniscus moved so slow that DNA molecules not only accumulated at the anchored DNA spoke sites to serve as nucleation sites, but also along the drying front connecting two adjacent spokes. As a result, two spokes were merged together by forming a junction after the meniscus receding. At $T = 71$ °C (Figure S2e), stretched DNA spokes were obtained; however, the regularity of surface pattern in terms of the spacing between two adjacent spokes was reduced due to the increase of fingering instabilities.[32,33] An optimal temperature, $T = 65$ °C was identified, at which the meniscus receded neither too slow causing two neighboring DNA spokes to merge together, nor too fast so that the regularity of parallel spokes decreased. The ranges of both temperature and pH that rendered the production of highly aligned DNA spokes were summarized in Figure S3, providing an important piece of information on the proper selection of these two variables to yield well-ordered and positioned DNA that can be used for further research.

Quite interestingly, rather than spokes yielded from dynamic self-assembly of DNA in sphere-on-flat geometry, a set of parallel stripes were formed by allowing the DNA solution to evaporate in cylinder-on-flat geometry composed of a cylindrical lens situated on a PDMS substrate (Figure 4). It is worth noting that in comparison to spokes, highly ordered parallel DNA stripes with much fewer junctions over a large area were obtained in cylinder-on-flat geometry (Figure 4c). The ability to integrate a large number of one-dimensional DNA stripes into 2D arrays is key to functional DNA-based devices. By performing two orthogonal transfer printing as illustrated in Figure 5a, 2D arrays of DNA nanowires can be achieved. First, parallel DNA stripes were formed on a flat PDMS stamp by evaporative self-assembly of DNA. The use of PDMS substrate rather than PMMA allowed subsequent transfer of stretched DNA to a variety of surfaces through transfer printing (TP) to form complex patterns. After first TP of DNA onto the Si substrate, the second TP was followed by placing DNA stripes in the direction orthogonal to the first TP patterns, thereby yielding 2D arrays of DNA nanowires (Figure 5b). The AFM measurement showed that the height of two crossed DNA stripes in the overlapped area after two consecutive TPs was approximately 60 nm, and was not the simple sum of the height of stripe 1 (40 nm) and stripe 2 (30 nm), indicating that DNA molecules in each stripe were not tightly bundled (*i.e.*, packed) but with possible spacing among them. Upon the addition of orthogonal DNA stripes on the existing ones, the height decreased. These 2D arrays of DNA nanowires may be used for the construction of functional circuits of DNA-based nanostructures by functionalizing DNA with electronically, magnetically, or chemically active materials;[19] moreover, more complex DNA patterns may be created by multiple TPs. This work is currently underway.

CONCLUSIONS

In summary, we demonstrated a simple and low-cost strategy based on controlled evaporative self-assembly in axially symmetric curve-on-flat geometry to yield a high number density of aligned long DNA nanowires (spokes and parallel stripes) over a macroscopic area (*i.e.*, millimeter scale). The pH of the DNA solution and temperature were found to be important variables that markedly influenced surface patterns of DNA deposits. Such highly oriented DNA nanowires and 2D arrays constructed upon them may provide opportunities to realize the potential of DNA-based nanotechnology for a large-scale production of high-density functional nanodevices by capitalizing on these aligned insulating DNA patterns as template.

EXPERIMENTAL SECTION

Preparation of PMMA-Coated Si Substrate. A p-type Si wafer (100) was cut into small 1.5−2 cm^2 pieces. These pieces were then cleaned with a mixed solution of 18 M sulfuric acid and NoChromix for 12 h. After the acid treatment, Si wafer was then vigorously rinsed with DI water and blow-dried with N_2. A layer of hexamtheyldisilazane (HMDS) was spun on Si substrate at 3000 rpm for 60 s, followed by the spin-coating of poly(methylmethacrylate) (PMMA; Polymer Source, Inc.; molecular weight, $MW_{PMMA} = 533$ kg/mol, PDI = 1.57) toluene solution at a concentration of 4 mg/mL at 2000 rpm for 60 s. The resulting PMMA-coated Si substrates (*i.e.*, thin PMMA film deposited on HMDS-coated Si) were annealed at 120 °C for 1 h and allowed to cool to room temperature before use.

Preparation of λ-DNA Buffer Solution. For the preparation of λ-DNA buffer solution, 1 M HCl solution was first prepared by diluting 16.53 mL of 12.1 M HCl stock solution to 200 mL with ultrapure H_2O. A total of 0.588 g (0.002 mol) of trisodium citrate dihydrate (TCD) (Fisher Scientific) and 0.5840 g of ethylenediaminetetraacetic acid (EDTA) (FisherBiotech electrophoresis grade, MW = 292.24) were added to 190 mL of ultrapure H_2O. By adding HCl solution to the TCD/EDTA buffer solution, various pH's (*i.e.*, pH = 4.7, 5.1, 5.5, 5.8, 6.2, 6.4, 6.7, and 7.1) were measured and adjusted using a calibrated pH probe. The solution was stirred for 1 h. λ-DNA (New England Biolabs; 48 502 bp; 500 μg/mL in 10 mM Tris·HCl/1 mM EDTA; pH ≈ 8.0) was directly added into the buffer solution described above in a 1.7 mL hinged-cap plastic microvial to yield 8 μg/mL DNA solution. To fluorescently label λ -DNAs at a dye/base-pair ratio of 1:15, YOYO-1 iodide (Life Technologies Corporation, 3 μL) was directly taken from the original solution and added to 8 μg/mL λ -DNA solution (2.4 mL). All procedures were conducted in the dark to prevent the dyes from bleaching. Finally, a green-emitting λ -DNA solution was yielded.

Controlled Evaporative Self-Assembly of DNA Buffer Solution in Curve-on-Flat Geometry. To construct a confined geometry (*i.e.*, curve-on-flat

geometry) that was composed of either a spherical lens (*i.e.*, sphere-on-flat) or a cylindrical lens (*i.e.*, cylinder-on-flat) on a flat substrate, a spherical lens made from fused silica and a PMMA-coated Si substrate (for sphere-on-flat), and a cylindrical lens made from fused silica and a PDMS substrate (for cylinder-on-flat) were used. The diameter of spherical lens *D* was 1 cm (Figure 1a). The diameter and the length of cylindrical lens were 1 and 1 cm, respectively (Figure 4a). The contact of the spherical lens or cylindrical lens with PMMA-coated Si substrate was made using a computer programmable inchworm motor with a step motion on the micrometer scale. Prior to the loading of DNA solution in curve-on-flat geometry, the 1.7 mL microvials containing a specified DNA concentration were submerged in a 37 °C water bath for 10−15 min to ensure homogeneity of λ-DNA in solution. The PMMA-coated Si substrate was heated on a Linkam Scientific Precision Temperature Controlled Microscope Stage (Linkam TMS 94 LTS 350) at different temperatures (*e.g.*, 55, 65, and 71 °C). The humidity was controlled to be the same throughout all experiments. The evaporation took approximately 30 min to complete. Only the patterns formed on the PMMA-coated Si substrate were evaluated by optical microscope (OM; Olympus BX51) and AFM (Dimension 3100 (Digital Instruments) scanning force microscope in tapping mode).

Conflict of Interest: The authors declare no competing financial interest.

Acknowledgment. We gratefully acknowledge support from the National Science Foundation (NSF CMMI-1153663) and Georgia Institute of Technology.

Supporting Information Available: The fluctuations in height along two DNA spokes, and summary of experimental results on the formation of DNA spokes at various pHs and temperatures. This material is available free of charge *via* the Internet at http://pubs.acs.org.

REFERENCES AND NOTES

1. Bensimon, A.; Simon, A.; Chiffaudel, A.; Croquette, V.; Heslot, F.; Bensimon, D. Alignment and Sensitive Detection of DNA by a Moving Interface. *Science* **1994**, *265*, 2096–2098.
2. Becerril, H. A.; Woolley, A. T. DNA-Templated Nanofabrication. *Chem. Soc. Rev.* **2009**, *38*, 329–337.
3. Hopkins, D. S.; Pekker, D.; Goldbart, P. M.; Bezryadin, A. Quantum Interference Device Made by DNA Templating of Superconducting Nanowires. *Science* **2005**, *308*, 1762–1765.
4. O'Carroll, D.; Lieberwirth, I.; Redmond, G. Microcavity Effects and Optically Pumped Lasing in Single Conjugated Polymer Nanowires. *Nat. Nanotechnol.* **2007**, *2*, 180–184.
5. Wang, J.; Gudiksen, M. S.; Duan, X.; Cui, Y.; Lieber, C. M. Highly Polarized Photoluminescence and Photodetection from Single Indium Phosphide Nanowires. *Science* **2001**, *293*, 1455–1457.
6. Hu, M.-S.; Chen, H.-L.; Shen, C.-H.; Hong, L.-S.; Huang, B.-R.; Chen, K.-H.; Chen, L.-C. Photosensitive Gold-Nanoparticle-Embedded Dielectric Nanowires. *Nat. Mater.* **2006**, *5*, 102–106.
7. Keren, K.; Berman, R. S.; Buchstab, E.; Sivan, U.; Braun, E. DNA-Templated Carbon Nanotube Field-Effect Transistor. *Science* **2003**, *302*, 1380–1382.
8. Hsieh, C.-H.; Chou, L.-J.; Lin, G.-R.; Bando, Y.; Golberg, D. Nanophotonic Switch: Gold-in-Ga_2O_3 Peapod Nanowires. *Nano Lett.* **2008**, *8*, 3081–3085.
9. Wang, H.; Muren, N. B.; Ordinario, D.; Gorodetsky, A. A.; Barton, J. K.; Nuckolls, C. Transducing Methyltransferase Activity into Electrical Signals in a Carbon Nanotube-DNA Device. *Chem. Sci.* **2012**, *3*, 62–65.
10. Hamedi, M.; Elfwing, A.; Gabrielsson, R.; Inganäs, O. Electronic Polymers and DNA Self-Assembled in Nanowire Transistors. *Small* **2013**, *9*, 363–368.
11. Chien, C.-C.; Velizhanin, K.; Dubi, Y.; Zwolak, M. Tunable Thermal Switching *via* DNA-Based Nano-Devices. *Nanotechnology* **2013**, *24*, 095704.
12. Li, T.; Zhang, L.; Ai, J.; Dong, S.; Wang, E. Ion-Tuned DNA/Ag Fluorescent Nanoclusters as Versatile Logic Device. *ACS Nano* **2011**, *5*, 6334–6338.
13. Deng, Z.; Mao, C. DNA-Templated Fabrication of 1d Parallel and 2d Crossed Metallic Nanowire Arrays. *Nano Lett.* **2003**, *3*, 1545–1548.
14. Dewarrat, F.; Calame, M.; Schönenberger, C. Orientation and Positioning of DNA Molecules with an Electric Field Technique. *Single Mol.* **2002**, *3*, 189–193.
15. Yokota, H.; Sunwoo, J.; Sarikaya, M.; van den Engh, G.; Aebersold, R. Spin-Stretching of DNA and Protein Molecules for Detection by Fluorescence and Atomic Force Microscopy. *Anal. Chem.* **1999**, *71*, 4418–4422.
16. Petit, C. A. P.; Carbeck, J. D. Combing of Molecules in Microchannels (Commic): A Method for Micropatterning and Orienting Stretched Molecules of DNA on a Surface. *Nano Lett.* **2003**, *3*, 1141–1146.
17. Michalet, X.; Ekong, R.; Fougerousse, F.; Rousseaux, S.; Schurra, C.; Hornigold, N.; Slegtenhorst, M. v.; Wolfe, J.; Povey, S.; Beckmann, J. S.; Bensimon, A. Dynamic Molecular Combing: Stretching the Whole Human Genome for High-Resolution Studies. *Science* **1997**, *277*, 1518–1523.
18. Allemand, J. F.; Bensimon, D.; Jullien, L.; Bensimon, A.; Croquette, V. Ph-Dependent Specific Binding and Combing of DNA. *Biophys. J.* **1997**, *73*, 2064–2070.
19. Guan, J.; Lee, L. J. Generating Highly Ordered DNA Nanostrand Arrays. *Proc. Nati. Acad. Sci. U.S.A.* **2005**, *102*, 18321–18325.
20. Guan, J.; Yu, B.; Lee, L. J. Forming Highly Ordered Arrays of Functionalized Polymer Nanowires by Dewetting on Micropillars. *Adv. Mater.* **2007**, *19*, 1212–1217.
21. Nakao, H.; Taguchi, T.; Shiigi, H.; Miki, K. Simple One-Step Growth and Parallel Alignment of DNA Nanofibers *via* Solvent Vapor-Induced Buildup. *Chem. Commun.* **2009**, 1858–1860.
22. Han, W.; Lin, Z. Learning from "Coffee Rings": Ordered Structures Enabled by Controlled Evaporative Self-Assembly. *Angew. Chem., Int. Ed.* **2012**, *51*, 1534–1546.
23. Byun, M.; Bowden, N. B.; Lin, Z. Hierarchically Organized Structures Engineered from Controlled Evaporative Self-Assembly. *Nano Lett.* **2010**, *10*, 3111–3117.
24. Hong, S. W.; Byun, M.; Lin, Z. Robust Self-Assembly of Highly Ordered Complex Structures by Controlled Evaporation of Confined Microfluids. *Angew. Chem., Int. Ed.* **2009**, *121*, 520–524.
25. Hong, S. W.; Wang, J.; Lin, Z. Evolution of Ordered Block Copolymer Serpentines into a Macroscopic, Hierarchically Ordered Web. *Angew. Chem., Int. Ed.* **2009**, *121*, 8506–8510.
26. Hong, S. W.; Xia, J.; Lin, Z. Spontaneous Formation of Mesoscale Polymer Patterns in an Evaporating Bound Solution. *Adv. Mater.* **2007**, *19*, 1413–1417.
27. Xu, J.; Xia, J.; Lin, Z. Evaporation-Induced Self-Assembly of Nanoparticles from a Sphere-on-Flat Geometry. *Angew. Chem., Int. Ed.* **2007**, *119*, 1892–1895.
28. Leizerson, I.; Lipson, S. G.; Lyushnin, A. V. Finger Instability in Wetting−Dewetting Phenomena. *Langmuir* **2003**, *20*, 291–294.
29. Zhang, J.; Ma, Y.; Stachura, S.; He, H. Assembly of Highly Aligned DNA Strands onto Si Chips. *Langmuir* **2005**, *21*, 4180–4184.
30. Kim, J. H.; Shi, W.-X.; Larson, R. G. Methods of Stretching DNA Molecules Using Flow Fields. *Langmuir* **2007**, *23*, 755–764.
31. Satti, A.; Aherne, D. Fitzmaurice. Analysis of Scattering of Conduction Electrons in Highly Conducting Bamboolike DNA-Templated Gold Nanowires. *Chem. Mater.* **2007**, *19*, 1543–1545.
32. Huang, J.; Kim, F.; Tao, A. R.; Connor, S.; Yang, P. D. Spontaneous Formation of Nanoparticle Stripe Patterns through Dewetting. *Nat. Mater.* **2005**, *4*, 896–900.
33. Xu, J.; Xia, J.; Hong, S. W.; Lin, Z.; Qiu, F.; Yang, Y. Self-Assembly of Gradient Concentric Rings *via* Solvent Evaporation from a Capillary Bridge. *Phys. Rev. Lett.* **2006**, *96*, 066104.

34. Herrick, J.; Bensimon, A. Invited Review. Imaging of Single DNA Molecule: Applications to High-Resolution Genomic Studies. *Chromosome Res.* **1999**, *7*, 409–423.
35. Deegan, R. D. Pattern Formation in Drying Drops. *Phys. Rev. E* **2000**, *61*, 475–485.